

# Design and Control of a 7-degree-of-freedom Symmetric Manipulator Module for In-Orbit Operations

Irene Cotrina de los Mozos  
MSc Robotics  
Cranfield University  
Cranfield, United Kingdom  
i.cotrinadelosmozos.212@cranfield.ac.uk

Dr. Gilbert Tang  
Centre for Robotics and Assembly  
Cranfield University  
Cranfield, United Kingdom  
g.tang@cranfield.ac.uk

**Abstract**— This paper proposes a modular redesign of multi-armed robotic systems with application to in-orbit operations. The manipulators that the robot includes are made independent and the connection to the central body is achieved through additional standard interfaces (SI). This grants the system the ability to self-repair through self-reconfiguration. The arms are also upgraded, giving rise to symmetrical manipulators of 7 degrees of freedom (DOF) capable of locomoting by themselves. The models of the new manipulator design are presented along with its nominal workspace. In addition to this, a novel algorithm for the control of the arm is developed based on the FABRIK approach. This programme is tested using diverse target poses as input and the consequent results are shown too. All the models and sketches were created in SolidWorks; the algorithm was coded in MATLAB.

**Keywords**— modular design, self-reconfiguration, FABRIK, inverse kinematics, control algorithm, SolidWorks, MATLAB

## I. INTRODUCTION

From its beginnings, Robotics has enabled the automation of processes that could be performed more efficiently by machines than by humans. The increased flexibility of mobile robots, in particular, make them suitable for countless applications where autonomous locomotion is required, such as transport or inspection. However, currently widespread mobile robots have fixed configurations and are not able to adapt to changing environments. In other cases, the substitution of the human workforce with robots might be desirable if the working environment poses a health risk.

Mobile modular robotics offers a solution to these concerns. Modularity refers to the property of systems that are composed of standardized units, which allow for an easy assembly. More importantly, this characteristic makes the system easily reconfigurable according to the varying needs; that is, the modules can be conveniently attached or detached to adapt to the environment or modify the functionalities of the whole. These modules can either be similar in design and capability (homogeneous) or dissimilar (heterogeneous) [1].

Concerning spatial applications, the harsh conditions in outer space are life-threatening to astronauts. Coupled with this, autonomous on-orbit assembly has been gaining interest recently due to the bypassing of limitations that traditional space structure construction has [2]. Once the structure is finished, additional operations of maintenance and even on-orbit servicing are sought-after [3]. Therefore, mobile modular robots

are an adequate option that can cover the needs of the entire mission.

This paper proposes an improved design to multi-armed systems for space assembly and operations based on modularity. These robots use their arms for locomotion on the structure being built as well as for manipulation of the modules that constitute it through standard interfaces (SI).

By treating each arm and the central torso as separate entities connected by SI, the resultant robot is modular and heterogeneous. This approach permits self-repair by self-reconfiguration in case of manipulator failure, as the main body can simply let go of the inoperative arm while a new one locomotes independently on the structure towards it and attaches both free SI together. The locomotion of the independent arm is performed by alternatively docking its two SI with that of the next structure module in the desired direction.

The rest of the report is structured as follows: Section II reviews relevant modular robotic projects with varied applications; Section III introduces the proposed new design; Section IV explains its control algorithm, and subsequently Section V presents the results obtained from testing; finally, Section VI concludes the paper.

## II. LITERATURE REVIEW

Modular robotics has gained popularity throughout the years due to the advantages it offers, mainly self-reconfiguration and the standardisation of units. This design approach aspires to overcome the limitations of traditional robots in an extensive range of fields.

The self-reconfigurable wave-like crawling (SWC) robot developed in [4], for example, aims to improve locomotion of current mobile robots by using a single motor for this purpose. This motor rotates a helix that, in turn, mobilises a chain of links located around it in an oscillatory manner. This unit also comprises the servomotors for the autonomous attachment and detachment of modules, both in parallel and in series, through 2 DOF joints. While the addition of modules in series helps the robot cross gaps and climb stairs, a second unit in parallel grants the steering capability if different speeds are commanded to the right and left modules.

Nature is often a reliable reference for mechanical designs, and that applies to modular robots as well. SnakeTrack is a bio-inspired mobile robot for surveillance and inspection on uneven terrain and in narrow spaces [7]. It is made up of a vertebral column and a track surrounding it; the former is composed of

two modules located on its ends and intermediate vertebrae. The length of the robot can be modified depending on the specific environment and necessary space for equipment by changing the number of vertebrae.

Each end module includes a camera for vision and two actuators. The former is fed an intermittent view as a result of the central openings of the track modules. Regarding the actuators, one moves the track for locomotion, and the other actuates lateral flexion for steering by pulling a rope that links with the opposite end module. Thus, the robot shifts towards the side of the pulled rope.

For industrial settings, the heterogeneous modular robot SABER offers various functions; in fact, its name stands for Step, Assembler, Bridge, Explorer Robot [5]. It is composed of a platform located on top of a rail which allow for three modes: monowheel, rail trolley and manipulator. The first configuration permits locomotion; the second is useful for overcoming gaps, climbing steps and getting through narrow paths; lastly, the third makes use of two arms of 7 degrees of freedom (DOF) to manipulate objects with tools.

The monowheel is generated by the two manipulators when their end links are attached together. Locomotion is achieved through a motor placed on the platform. These manipulators are also the rail on which the platform slides when they are extended, using the same motor. Their extreme links include androgenous interfaces that can dock with tools and other SABER manipulators. The platform also contains the control unit and four support legs for the rail to move relatively to it. For material handling, the objects to transport can be loaded on the platform and carried in the monowheel configuration.

Nevertheless, modular robots are not necessarily bound to the ground. Reference [6] presents a self-reconfigurable aerial vehicle for package delivery. Each module behaves as an individual mobile robot on the ground until the units get together. Then, they connect themselves to their adjacent module using a tethering system, and they surround the package and clamp onto it. At this point, the created UAV (Unmanned Aerial Vehicle) can take off.

The modules include the retractable tether with an end hook on one side, an also retractable claw that the hook can connect to on the other side, three omnivheels for locomotion on the

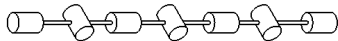


Fig. 1. Manipulator joint configuration.

ground, a rotor, and a compliant pad at the front that makes contact with the package. After tethering, the modules hold the payload on its flat sides with the compliant pads. A winch applies the necessary tension to keep the units together.

Examples of modular robots can be found in space technologies too. The Multi-arm Installation Robot for Ready ORUs and Reflectors project, or MIRROR for short, intends to develop a robotic system for the assembly of large modular structures on-orbit. Reference [8] takes a modular approach to the design of their MAR (Multi-Arm Robot), which consists of a central torso and two 7 DOF arms. These are functionally independent and are joined together through standard interfaces (SI).

Connections between the parts are achieved through HOTDOCK standard interfaces [9]. The two SI where the manipulators are attached are fixed, whereas the third, used for grabbing payload or docking with the structure, can rotate around its axis. The two arms are used for locomotion on the built structure and manipulation of the modules through the SI end-effectors.

The Modular Satellite Assembly and Reconfiguration (MOSAR) project, for its part, aims to develop a spacecraft system for in-space operations [11]. It comprises a set of cubic blocks and a symmetric manipulator. The cube modules are heterogeneous and tailored to fulfil a specific function each, whether it be sensing, thermal regulation, powering or control. The robotic arm is responsible for lattice reconfiguration with the objective of optimising the built spacecraft according to mission requirements; it handles and assembles the modules, while also being capable of locomoting on them to reposition itself. Mechanical, thermal, data and power connections (mechanical, thermal, data and power) for these purposes are achieved through SI.

Marsbee, on another note, is a modular system devised for exploratory missions on Mars [10]. It is composed of a rover that works as a base and a swarm of aerial Marbees. The latter include bio-inspired flapping wings designed to improve aerodynamics and consume little power. Because there are many of these bee-sized modules, the system proves robust to individual breakdowns. The Marsbees also carry communication devices and sensors, which results in the capacity to create reconfigurable sensor networks. They can collect data and samples of the Martian environment too. The rover, for its part, serves as charging point and communication centre.

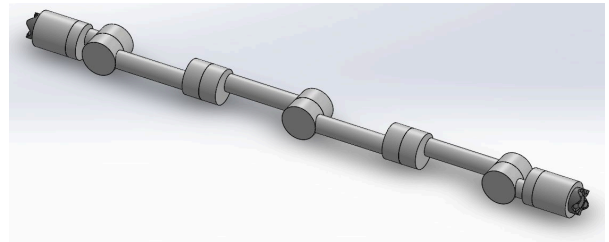


Fig. 2. Proposed manipulator model

### III. DESIGN

After adopting a modular design approach, the manipulators of the system are able to locomote independently. Therefore, the arms need to be redesigned to better adapt them to this added functionality.

Indeed, the new arms are symmetrical in their joint configuration, which simplifies their kinematics during the crawling motion. While locomoting, the manipulator reaches for the SI of the next structure module with its own free SI. Once securely docked, the other SI detaches and follows the same mode of operation. Thus, what is considered as base and end-effector switch continuously between the two end links depending on what SI is docked at that moment. Symmetry facilitates the control of this motion as the same kind of kinematics equations or algorithm can be applied with no regard for the docked interface. On another note, because a single manipulator must locomote on the structure by itself, its reach has to allow it to dock with adjacent modules. Additionally, both ends should contain spherical wrists for the precise positioning of the end-effector. It is also preferable that the arm be able to reach below its base plane for greater flexibility.

The resultant manipulator is a 7 DOF arm of revolute joints, with pivot and hinge joints positioned in an alternative manner. This configuration is visualised in Fig. 1. Its total length without considering the SI is 1600mm; this is a compromise between adequate reach and moderate length in favour of precision. A model of the manipulator can be seen in Fig. 2, and Fig. 3 shows its nominal workspace assuming a 130° limit for the hinge joints.

### IV. CONTROL ALGORITHM

The algorithm for the control of the 7 DOF manipulator is based on the Forward and Backward Reaching Inverse Kinematics method, also known as FABRIK for short [12]. Precisely, this approach is adapted to serial manipulators, as done previously in [13], and tailored to the proposed arm. As its name implies, there are two phases: the forward stage and the

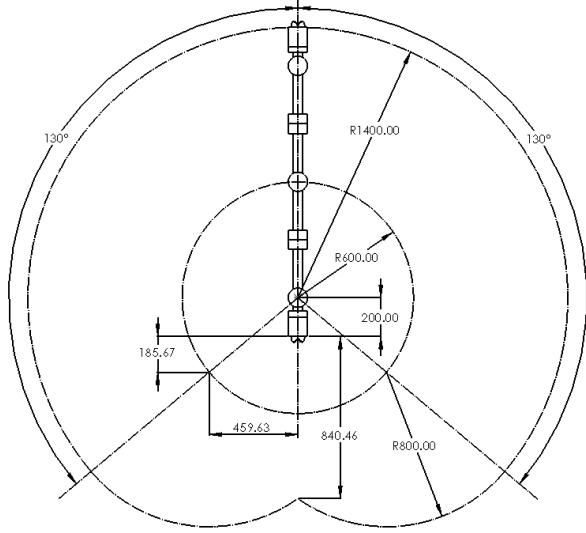


Fig. 3. Manipulator nominal workspace.

backward stage. The former involves assuming the end-effector has reached the goal pose, and therefore the calculation of each previous joint's position, frame and value partially relies on the information of the subsequent one; the latter is its parallel, only returning the first joint to its base, so that data from subsequent joints is based on the knowledge about the previous joint. These phases are repeated until the RMSE fulfils the specified stopping criteria.

Knowing that each joint is assigned a reference frame in such a way that pivot joints rotate around their Z axis and hinge joints rotate around their X axis, some general rules can be noted. As a result of this frame assignment, pivot joints do not have the ability to reorient their Z axis, so they "inherit" the Z axis of the previous hinge joint. In the same way, hinge joints cannot alter their X axis, and thus it is the same as that of the previous pivot joint.

Now, the steps to complete these two phases are detailed, depending on the type of joint under study. A single apostrophe refers to the data updated in the forward stage, whereas two apostrophes imply a new value in the backward stage. The axes of the frames are denoted as x, y and z, l is a link length, p means position of a joint, and q its value. It is assumed that pivot joints do not have an angular limit

#### A. Forward stage

##### a) Hinge joint $i$

The Z axis of the hinge joint is given by that of its next pivot joint. With that information, the new position of the former can be calculated:

$$z'_i = z'_{i+1} \quad (1)$$

$$p'_i = p'_{i+1} - l_i z'_i \quad (2)$$

Its X axis is perpendicular to the plane defined by its own Z axis and that of the previous pivot joint. Then, the latter Z axis must be calculated first, which is equal to the Z axis of the hinge joint that precedes it. This direction is determined by the vector  $d$  that connects the hinge joint that comes before and the one under study, whose position has just been updated.

$$d = p'_i - p_{i-2} \quad (3)$$

$$z'_{i-1} = z'_{i-2} = \frac{d}{|d|} \quad (4)$$

$$x'_i = \frac{z'_i \times z'_{i-1}}{|z'_i \times z'_{i-1}|} * \text{sign}(x'_i \cdot x_i) \quad (5)$$

If the denominator turns out to be 0 ( $z'_i$  and  $z'_{i-1}$  are parallel),  $x'_i$  is taken as  $x'_{i+1} * \text{sign}(x'_i \cdot x_i)$ . In these cases, the sign function prevents unexpected flipping of the X axis as stated in [13]. It is omitted in the cases where it is equal to 0 (new X axis perpendicular to old one).

At this point, the Y axis can be obtained from the cross product of Z and X, and the joint value of the posterior pivot joint can be calculated from its definition.

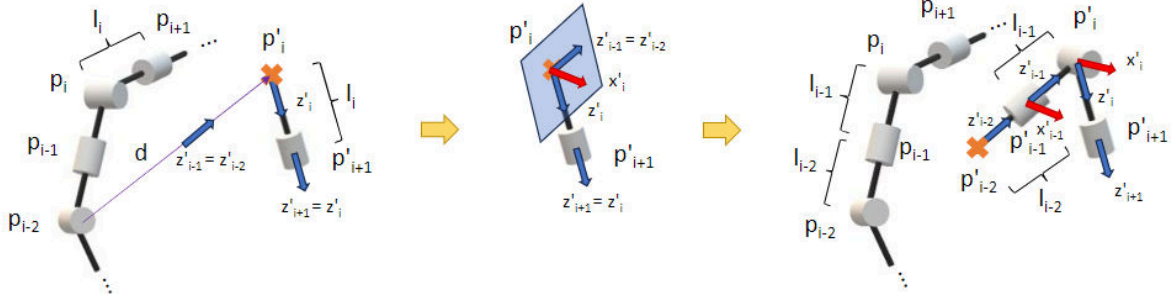


Fig. 4. Forward stage steps.

$$y'_i = z'_i \times x'_i \quad (6)$$

$$q'_{i+1} = \cos^{-1}(x'_i \cdot x'_{i+1}) * \text{sign}((x'_i \times x'_{i+1}) \cdot z'_i) \quad (7)$$

#### b) Pivot joint $i$

Knowing its Z axis, the updated position of the pivot joint can be obtained, and its X axis is given by that of the next hinge joint. Thus, the Y axis can be known too.

$$p'_i = p'_{i+1} - l_i z'_i \quad (8)$$

$$x'_i = x'_{i+1} \quad (9)$$

$$y'_i = z'_i \times x'_i \quad (10)$$

The joint value of the posterior hinge joint is then calculated in a similar fashion as in (7).

$$q'_{i+1} = \cos^{-1}(z'_i \cdot z'_{i+1}) * \text{sign}((z'_i \times z'_{i+1}) \cdot x'_i) \quad (11)$$

If the limit for the hinge joint is exceeded, it is set to that maximum value ( $q_L$ ), and the Z and Y axes are recalculated together with the joint position:

$$q'_{i+1} = q_L * \text{sign}(q'_{i+1}) \quad (12)$$

$$z'_i = z'_{i+1} * \cos(q_{i+1}) + y'_{i+1} * \sin(q_{i+1}) \quad (13)$$

$$y'_i = z'_i \times x'_i \quad (14)$$

$$p'_i = p'_{i+1} - l_i z'_i \quad (15)$$

$$z'_{i-1} = z'_i \quad (16)$$

When the base is reached, the joint value of the first pivot joint is calculated with respect to the global X axis,  $[1 \ 0 \ 0]$ .

These steps are visualized in Fig. 4.

### B. Backward stage

#### a) Hinge joint $i$

Since the information from the previous pivot joint is known, the updated position of the hinge joint is obtained:

$$p''_i = p''_{i-1} + l_{i-1} z''_{i-1} \quad (17)$$

Now, the Z axis is set as the unit vector pointing towards the next hinge joint, whose position has not yet been updated:

$$d = p'_{i+2} - p''_i \quad (18)$$

$$z''_i = \frac{d}{|d|} \quad (19)$$

Next, the X axis is determined in an equivalent way as the one explained in the forward stage:

$$x''_i = \frac{z''_i \times z''_{i-1}}{|z''_i \times z''_{i-1}|} * \text{sign}(x''_i \cdot x'_i) \quad (20)$$

If the denominator happened to be zero,  $x''_i$  is taken as  $x''_{i-2} * \text{sign}(x''_i \cdot x'_i)$ , or  $[1 \ 0 \ 0]$  for the first hinge joint. With both Z and X, the Y axis is obtained. Since the hinge joint's X axis is set by its previous pivot joint, the frame for the latter joint is known too.

$$y''_i = z''_i \times x''_i \quad (21)$$

$$x''_{i-1} = x''_i \quad (22)$$

$$y''_{i-1} = z''_{i-1} \times x''_{i-1} \quad (23)$$

Finally, the joint values for both the hinge joint and the pivot joint that comes before it can be obtained:

$$q''_{i-1} = \cos^{-1}(x''_{i-2} \cdot x''_{i-1}) * \text{sign}((x''_{i-2} \times x''_{i-1}) \cdot z''_{i-2}) \quad (24)$$

$$q''_i = \cos^{-1}(z''_{i-1} \cdot z''_i) * \text{sign}((z''_{i-1} \times z''_i) \cdot x''_{i-1}) \quad (25)$$

Again, if limit for the hinge joint value is exceeded, it takes that maximum value, and the frame is recalculated:

$$q''_i = q_L * \text{sign}(q''_i) \quad (26)$$

$$z''_i = z''_{i-1} * \cos(q''_i) - y''_{i-1} * \sin(q''_i) \quad (27)$$

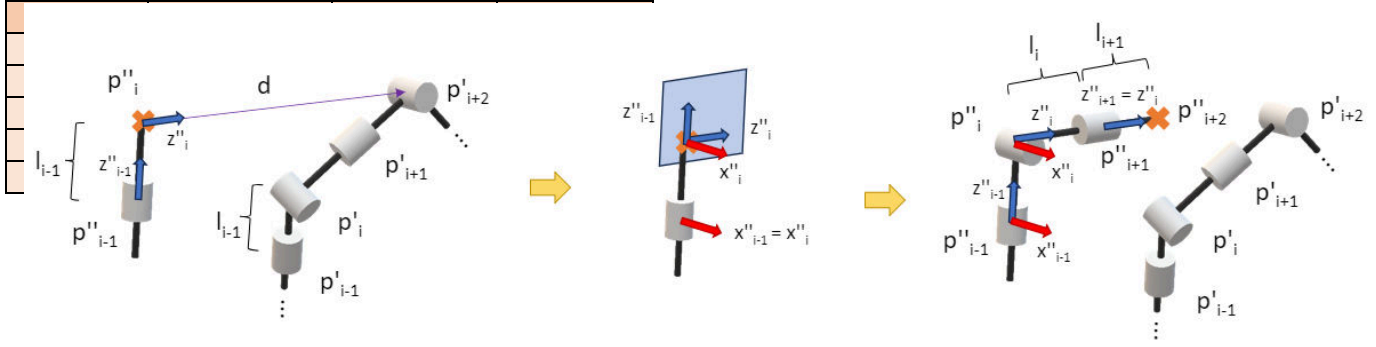


Fig. 5. Backward stage steps.

TABLE II. RESULTS OF TESTS

TABLE I. TARGET POSES

Case	Target position [m]			Target orientation		
	x	y	z	X	Y	Z
1	0	1.135	0	[1 0 0]	[0 -1 0]	[0 0 -1]
2	0.500	0.500	0.500	[1 0 0]	[0 -1 0]	[0 0 -1]
3	-0.300	-0.400	-0.100	[-0.707 -0.707 0]	[-0.707 0.707 0]	[0 0 -1]
4	0	0.141	1.259	[1 0 0]	[0 -0.707 -0.707]	[0 0.707 -0.707]
5	0	0	-1.400	[1 0 0]	[0 -1 0]	[0 0 -1]

$$y''_i = z''_i \times x''_i \quad (28)$$

#### b) Pivot joint $i$

The only unknowns left are the Z axis, which is set by the previous hinge joint, and the new position, which can be easily calculated with this last piece of information.

$$z''_i = z''_{i-1} \quad (29)$$

$$p''_i = p''_{i-1} + l_{i-1}z''_{i-1} \quad (30)$$

Exceptionally, the orientation of the last pivot joint is set as the closest possible to the target X axis, minding the orthogonality between axes:

$$x''_7 = \frac{x'_8 - (x'_8 \cdot z''_7)z''_7}{|x'_8 - (x'_8 \cdot z''_7)z''_7|} \quad (31)$$

If the denominator were null,  $x''_7$  is assumed to be equal to  $x''_6$  ( $x'_8$  is parallel to  $z''_7$ ).

Again, these steps are shown graphically in Fig. 5.

## V. RESULTS

To verify the proper functioning of the algorithm, some tests involving the target poses in Table I are performed. Starting from the home position (arm extended vertically), Case 1 aims to reach what would be the next docking interface; Cases 2 and 3 are other reachable examples; Cases 4 and 5, however, contemplate configurations that the manipulator is not capable of achieving due to the 130° hinge joint limit. The stopping criteria is set to a RMSE below 0.001 (as defined in [13]), or 200 iterations.

The results are collected in Table II, and the robotic arm is visualised in the corresponding configurations in Fig.6. In the first three cases, the RMSE drops below the threshold in just a few iterations. When it comes to the last two targets, although the end-effector does not reach the goal, the algorithm gives the closest possible configuration.

## VI. CONCLUSIONS AND FUTURE WORK

This report implemented modularity on multi-armed robots developed for in-orbit operations by making the arms independent of the torso to which they connect. In doing so, the system gains the ability to repair itself through self-reconfiguration. This is achieved through the locomotion of an independent manipulator towards the main body and its attachment to the latter in substitution of the broken-down arm. The original manipulator was redesigned to better adapt to its

assigned tasks, and the algorithm for its control was detailed. The tests performed show the reliability of the programme.

Nevertheless, it is fair to mention that the algorithm takes considerable time to run due to the high number of conditional blocks required to contemplate exceptional situations. Although this makes the programme more robust, the code should be optimised for computational efficiency. Future steps would include simulations showcasing the locomotion of the arm under the algorithm's control.

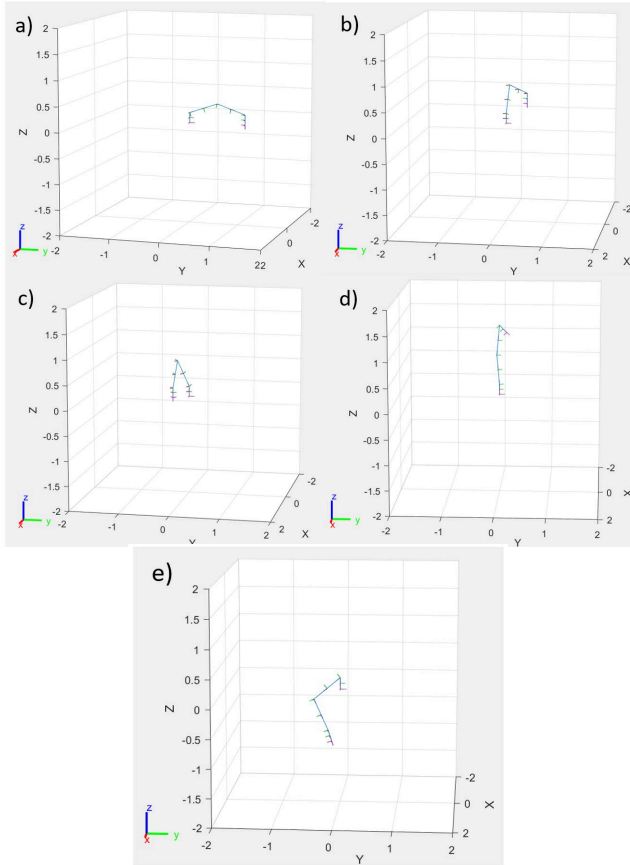


Fig. 6. Resultant manipulator configurations: a) Case 1; b) Case 2; c) Case 3; d) Case 4; e) Case 5.

## REFERENCES

- [1] W. Cheah et al., "MIRRAX: A Reconfigurable Robot for Limited Access Environments," *IEEE Transactions on Robotics*, Apr. 2022, doi: 10.1109/TRO.2022.3207095.
- [2] S. Bhadani, I. Cotrina, O. Pradhan, S. Dillikar, and A. Rajadurai, "SIMULATION OF AN ON-ORBIT MULTI-ROBOT ASSEMBLY SYSTEM," 2023.
- [3] J. P. Davis, J. P. Mayberry, and J. P. Penn, "ON-ORBIT SERVICING: INSPECTION, REPAIR, REFUEL, UPGRADE, AND ASSEMBLY OF SATELLITES IN SPACE," 2019.
- [4] H. Sun, Q. Wu, X. Wang, T. Yang, and N. Sun, "A New Self-Reconfiguration Wave-like Crawling Robot: Design, Analysis, and Experiments," *Machines*, vol. 11, no. 3, Mar. 2023, doi: 10.3390/machines11030398.
- [5] A. M. Romanov, V. D. Yashunskiy, and W. Y. Chiu, "SABER: Modular Reconfigurable Robot for Industrial Applications," in *IEEE International Conference on Automation Science and Engineering*, IEEE Computer Society, Aug. 2021, pp. 53–59. doi: 10.1109/CASE49439.2021.9551437.
- [6] Z. Imran, A. Scott, J. Buzzatto, and M. Liarokapis, "On the Development of Tethered, Modular, Self-Attaching, Reconfigurable Vehicles for Aerial Grasping and Package Delivery," in *SSRR 2022 - IEEE International Symposium on Safety, Security, and Rescue Robotics*, Institute of Electrical and Electronics Engineers Inc., 2022, pp. 1–6. doi: 10.1109/SSRR56537.2022.10018678.
- [7] S. E. Nodehi, L. Bruzzone, and P. Fanghella, "SnakeTrack, A Bio-inspired, Single Track Mobile Robot with Compliant Vertebral Column for Surveillance and Inspection," in *Mechanisms and Machine Science*, Springer Science and Business Media B.V., 2022, pp. 513–520. doi: 10.1007/978-3-031-04870-8\_60.
- [8] M. Deremetz et al., "DEMONSTRATOR DESIGN OF A MODULAR MULTI-ARM ROBOT FOR ON-ORBIT LARGE TELESCOPE ASSEMBLY."
- [9] M. A. Roa et al., "HOTDOCK: Design and Validation of a New Generation of Standard Robotic Interface for On-Orbit Servicing." [Online]. Available: <https://www.researchgate.net/publication/344871962>
- [10] C. Kang, "Marsbee - Swarm of Flapping Wing Flyers for Enhanced Mars Exploration," *nasa.gov*, Mar. 30, 2018.
- [11] "MOSAR: MODular Spacecraft Assembly and Reconfiguration," *h2020-mosar.eu*.
- [12] A. Aristidou and J. Lasenby, "FABRIK: A fast, iterative solver for the Inverse Kinematics problem," *Graph Models*, vol. 73, no. 5, pp. 243–260, Sep. 2011, doi: 10.1016/j.gmod.2011.05.003.
- [13] L. A. O. Moreno and J. H. A. Alcantara, "An adaptation of FABRIK algorithm for serial robot's inverse kinematics," in *2022 IEEE International Conference on Engineering Veracruz, ICEV 2022*, Institute of Electrical and Electronics Engineers Inc., 2022. doi: 10.1109/ICEV56253.2022.9959663.

2024-01-01

# Design and control of a 7-degree-of-freedom symmetric manipulator module for in-orbit operations

Cotrina de los Mozos, Irene

IEEE

---

de los Mozos IC, Tang G. (2024) Design and control of a 7-degree-of-freedom symmetric manipulator module for in-orbit operations. In: 2023 11th International Conference on Control, Mechatronics and Automation (ICCMA), 1-3 November 2023, Grimstad, Norway, pp. 284-289  
<https://doi.org/10.1109/ICCMA59762.2023.10374943>

*Downloaded from Cranfield Library Services E-Repository*